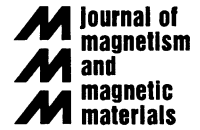




ELSEVIER

Journal of Magnetism and Magnetic Materials 223 (2001) 221–232



www.elsevier.com/locate/jmmm

Growth-induced perpendicular magnetic anisotropy and clustering in $\text{Ni}_x\text{Pt}_{1-x}$ alloys

D. Vasumathi, A.L. Shapiro, B.B. Maranville, F. Hellman*

Physics Department, University of California San Diego, La Jolla, CA 92093, USA

Received 30 August 2000; received in revised form 10 November 2000

Abstract

Polycrystalline and epitaxial (100), (110), and (111)-oriented Ni_3Pt , NiPt , and NiPt_3 films were deposited over a range of growth temperatures from 80°C to 700°C. Films grown at moderate temperatures (200–400°C) exhibit growth-induced properties similar to Co–Pt alloys: enhanced and broadened Curie temperature, perpendicular magnetic anisotropy and large coercivity. As in Co–Pt, the magnetic properties suggest a clustering of Ni into platelets on the growth surface, as the films are being grown. Unlike Co–Pt, however, NiPt films exhibit a strong orientational dependence of anisotropy and enhanced Curie temperature, possibly resulting from different types of surface reconstructions which affect the growth surface. © 2001 Elsevier Science B.V. All rights reserved.

Keywords: Ni–Pt alloy films; Perpendicular anisotropy; Growth induced; Ni platelets; Surface reconstruction

1. Introduction

Perpendicular magnetic anisotropy (PMA) is found in a number of transition metal alloys prepared by vapor deposition [1–15]. Although certain compositions of these alloys have oriented tetragonal or hexagonal phases where uniaxial anisotropy might be expected, [1,13,14] PMA has also been found over a wide compositional range in materials that should have cubic symmetry [2–12]. In particular, large PMA found in Co–Pt alloys which are FCC by both X-ray and TEM measurements has been attributed to a growth-induced effect, similar to amorphous Tb–Fe alloys

[4,7,8,12,15,16]. PMA exists in Pt-rich $\text{Co}_x\text{Pt}_{1-x}$ films prepared by both e-beam evaporation and sputtering, independent of crystallographic orientation and strain [9,12]. The magnitude of this anisotropy can be a significant fraction ($\sim 10\%$) of the anisotropy found in the best Co/Pt and Co/Pd multilayers. Various observations, including magnetic evidence of inhomogeneity, enhanced magnetic moment and magnetic onset temperature, EXAFS and angle-dependent magnetic circular dichroism experiments, suggest that the source of the anisotropy is a clustering of the Co within a Pt-rich matrix, in particular, in the form of Co platelets within an FCC Pt-rich matrix [8,11,12,17–19]. The cause of this clustering is not well understood, but appears to be an equilibrium surface effect, possibly related to surface segregation, which is then kinetically trapped into the growing film [7,8,12].

*Corresponding author.

E-mail addresses: vdharma@physics.ucsd.edu (D. Vasumathi), fhellman@ucsd.edu (F. Hellman).

The Ni–Pt alloy system is in many ways analogous to Co–Pt, but with significantly reduced Curie temperatures and hence magnetic interaction energy, thus providing a test of whether magnetic energy is relevant to the growth-induced clustering seen in Co–Pt. Ni/Pt multilayers have been reported to have PMA under some growth conditions [20–23]. At high temperature, in equilibrium, $\text{Ni}_x\text{Pt}_{1-x}$ alloys have a face centered cubic (FCC) structure for all Ni concentrations and are continuously soluble (A1 phase) [24,25]. At lower temperatures, long-range chemical order develops. Below 650°C near the NiPt composition, $\text{Ni}_x\text{Pt}_{1-x}$ exhibits Cu–Au type ($L1_0$) long-range order (LRO). Below 550°C near the Ni_3Pt composition and below 510°C near the NiPt_3 composition, $\text{Ni}_x\text{Pt}_{1-x}$ exhibits Cu_3Au type ($L1_2$) LRO. The $L1_0$ phase has a tetragonal distortion, but the $L1_2$ phase has cubic symmetry. Chemically disordered FCC Ni_3Pt has a Curie temperature of 115°C while the $L1_2$ phase has a Curie temperature of 20°C [24]. NiPt is known to magnetically order at 115 K in the chemically disordered FCC phase, but is paramagnetic in the completely ordered phase (the $L1_0$ phase). NiPt_3 is not magnetically ordered in any known bulk equilibrium phase [24].

Like Co–Pt, Ni–Pt alloys have been studied extensively for use in catalysis, and the structure of the alloy surfaces has been investigated in detail [26–31]. In equilibrium, $\text{Ni}_x\text{Pt}_{1-x}$ alloys are known to exhibit surface segregation [26–28]. For the (100) and (111) orientations, the top layer of NiPt is enhanced to between 75% and 90% Pt, while the second layer is depleted of Pt. Exponentially damped compositional oscillations extend four-to-six layers deep. The (110) orientation has the reverse segregation, with the top layer being Ni-rich and the second layer being Pt-rich [28]. The (111) orientation of NiPt has been measured by LEIS to be flat to within 0.05% [29], while the (100) orientation undergoes a shifted row reconstruction (as measured by STM) with every fifth row shifted up out of the plane [30], in contrast to (100) $\text{Co}_x\text{Pt}_{1-x}$ which undergoes a quasi-hexagonal surface net reconstruction [32]. High energy ion spectroscopy (HEIS) and LEED studies of ultra-thin Pt layers on Ni have shown that alloy

formation begins at 350°C, suggesting that bulk atomic diffusion is negligible below that temperature [31].

In this paper, we report results of (100), (110), (111), and polycrystalline epitaxial Ni_3Pt , NiPt and NiPt_3 films deposited at different substrate temperatures. We have performed vacuum annealing studies to verify the equilibrium state and to determine the contribution of growth-surface effects to the as-deposited magnetic properties of our samples. Structural characterization was done on a high-resolution X-ray diffractometer to study crystal quality and strain. $M(T)$ and $M(H)$ at various temperatures were measured in a SQUID, torque, or vibrating sample magnetometer to characterize the magnetic onset temperature, magnetization and anisotropy.

We find magnetic properties indicative of Ni clustering for all three film compositions deposited between 200°C and 400°C, a temperature range where the surface atomic mobility should be high and bulk atomic mobility low, similar to what was found in Co–Pt alloys. These properties include a broadened magnetic transition $M(T)$ with a significantly enhanced magnetization onset and in some cases $M(H)$ loops with large coercivity. For example, NiPt_3 films have an onset of magnetization of 80 K, despite being nonmagnetic in all known bulk phases, indicative of significant Ni clustering.

We find PMA in some as-deposited Ni–Pt alloy films. The largest PMA is found in (111) NiPt and Ni_3Pt films grown near 400°C, which also have the largest Ni clustering. We suggest that PMA originates in these films at the Ni/Pt interfaces of thin, flat Ni platelets in a Pt matrix, similar to the anisotropy found in deliberately prepared Ni/Pt multilayers. We find that in both NiPt and Ni_3Pt , unlike CoPt_3 , (100)-oriented samples exhibit significantly less PMA and less enhancement of the magnetic onset temperature than (111)-oriented samples. We attribute this difference to reduced Ni clustering possibly due to the difference in surface reconstruction between the two orientations altering the growth process. PMA vanishes with annealing at 450°C, indicative of a growth-induced effect, as in CoPt_3 films. NiPt_3 shows no sign of anisotropy.

2. Sample preparation and structural characterization

Epitaxial (1 0 0), (1 1 0), (1 1 1), and polycrystalline $\text{Ni}_x\text{Pt}_{1-x}$ films were grown on (1 0 0) MgO, (1 1 0) MgO, (0 0 0 1) Al_2O_3 , and amorphous-SiN-coated Si substrates, respectively. Samples were grown at deposition temperatures from 80°C to 700°C. Compositions $x \sim 0.25, 0.50$ and 0.75 were measured by electron microprobe ($x \pm 0.05$ is the variation in composition of samples; $x \pm 0.02$ is the microprobe uncertainty). The films were co-deposited from individual Ni and Pt electron beam evaporation sources. The total deposition rate was 0.5 Å/s and the pressure during deposition was 3.0×10^{-10} Torr. Film thickness varied between 2000 and 3700 Å and was determined with a force-sensitive profilometer.

Reflection high energy electron diffraction (RHEED) patterns were monitored during the growth of all films. NiPt and NiPt₃ samples showed vertical diffraction lines, with no sign of rings or diffuse scattering, indicative of epitaxial growth in both the (1 0 0) and (1 1 1) orientations. Ni₃Pt samples deposited directly onto Al_2O_3 and MgO were observed to produce circular ring diffraction patterns indicative of polycrystalline growth at all deposition temperatures. This is likely to be the result of the large lattice mismatch between the substrates and the sample at this composition. To achieve epitaxy for Ni₃Pt, we used a thin (~ 30 Å) Pt underlayer grown immediately before depositing the film.

High-resolution X-ray diffraction was used to characterize the films, particularly NiPt films which show PMA [33]. As-deposited NiPt films grown at 400°C show strong FCC peaks. As in CoPt₃, the inhomogeneity described below does not manifest itself in any unusual shape of the FCC peaks, which indicate a coherent structure with a single lattice constant. The (1 0 0) films show a weak (1 0 0) superlattice peak, which vanishes on annealing at 700°C (above the LRO temperature). The fwhm of the (1 1 1) peak in (1 1 1)-oriented films is 0.3°, corresponding to a structural coherence length of 200 Å (limited by defects or low angle grain boundaries, similar to that found in CoPt₃; see Ref. [12]). In samples grown or annealed at 700°C, the fwhm is

0.1°, indicating a structural coherence length of 600 Å. Lattice constants have been measured in the [3 3 1] and [3 1 1] directions of (1 1 1)-oriented NiPt samples deposited at 400°C and at 700°C, and deposited at 400°C and annealed at 700°C. An equivalent ‘in-plane’ lattice constant can be calculated from these off-axis peaks and a strain/tetragonal distortion computed between the perpendicular and in-plane lattice parameters. We find a tensile in-plane strain of $1.1 \pm 0.2\%$ in the sample grown at 400°C, which drops to $0.6 \pm 0.1\%$ after annealing at 700°C, and $0.2 \pm 0.1\%$ for the 700°C as-deposited sample. These strains are large compared to those seen in epitaxial CoPt₃ films ($<0.03\%$) [5,12].

3. Magnetic characterization

We have studied the magnetic transition, $M(T)$, in Ni₃Pt, NiPt, and NiPt₃ as a function of substrate temperature during growth T_s . Measurements at room temperature and above were done with a vibrating sample magnetometer (VSM). A calibrated Pt–Pt 13% Rh thermocouple was mounted directly on the quartz VSM sample rod and the rod was immersed in a temperature controlled flowing Ar gas. Measurements below room temperature were made in a SQUID magnetometer with temperature control achieved via flowing He gas. Each sample was first technically saturated in high field along the easy axis or easy plane of magnetization, then the applied field was reduced to 1000 Oe and the magnetization measured upon heating.

Fig. 1 shows the normalized $M(T)$ curves for several polycrystalline Ni₃Pt samples ($T_s = 200^\circ\text{C}, 400^\circ\text{C},$ and 650°C). Ni₃Pt films deposited at growth temperatures above its L1₂ order–disorder transition temperature (580°C) have a sharp magnetization transition and a magnetic onset temperature of 115°C, as expected for FCC Ni₃Pt. Ni₃Pt films grown between 200°C and 400°C have a broad magnetic transition and an increased onset temperature (by 30–85°C), indicative of Ni clustering, very similar to results previously seen for CoPt₃ [12]. Films grown at 80°C show a narrower magnetic transition with an onset slightly above the FCC Curie temperature of Ni₃Pt. Fig. 2 is a plot of the

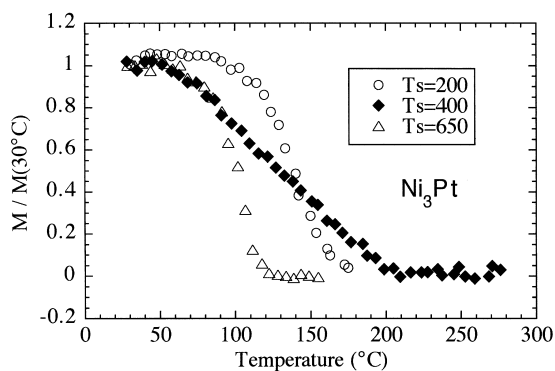


Fig. 1. Normalized $M(T)/M(30^\circ\text{C})$ vs. T for polycrystalline Ni_3Pt (~ 75 at% Ni) samples deposited at 200°C , 400°C , and 650°C . M for each film was measured on heating in 1000 Oe with H applied along the easy axis, after magnetically saturating at room temperature in 10000 Oe.

enhancement of the magnetic onset temperature above the corresponding FCC Curie temperature for each sample. Variations in composition of films grown at different temperatures were accounted for by subtracting the Curie temperature for the FCC structure at the composition (as determined by electron microprobe) of each sample.

Figs. 3a–c show $M(H)$ measured at room temperature for epitaxial (111), (100), and (110) Ni_3Pt grown at 385°C (compositions ~ 73 at% Ni). From room temperature torque measurements on the (111) sample, the intrinsic perpendicular anisotropy $K_{\text{ui}} = K_{\text{u}} + 2\pi M_{\text{s}}^2 = 1.3 \times 10^6 \text{ erg/cm}^3$, consistent with the $M(H)$ data. At 10 K, from $M(H)$, $K_{\text{ui}} = 3.5 \times 10^6 \text{ erg/cm}^3$ and $M_{\text{s}} = 370 \text{ emu/cm}^3$. For the (100) and (110) samples, $M(H)$ for H perpendicular and parallel saturate at similar fields. This indicates that there is a small perpendicular anisotropy; in H perpendicular M does not immediately saturate due to demagnetizing effects, i.e. formation of perpendicular domains in a relatively low coercivity material. Torque curves for the (100) sample show low overall anisotropy and indicate an inhomogeneous sample, with part of the sample having in-plane anisotropy and low coercivity and part having perpendicular anisotropy and higher coercivity. Polycrystalline samples show perpendicular anisotropy, but less strongly than might be expected given that they are textured (111).

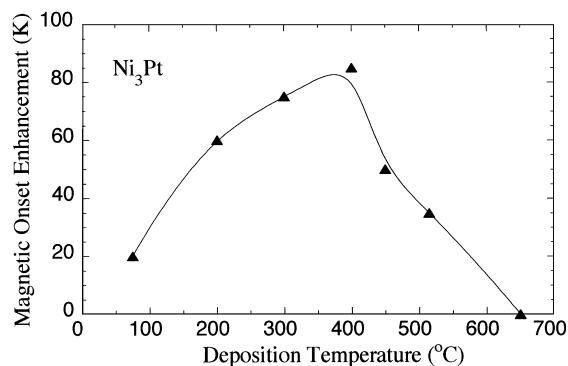


Fig. 2. Magnetic onset temperature T_{onset} enhancement of as-deposited polycrystalline Ni_3Pt films vs. substrate temperature during growth; T_{onset} is the temperature at which the magnetization drops to 5% of its value at 30°C . T_{onset} enhancement is T_{onset} minus the FCC Curie temperature of each sample at the measured composition (determined by electron microprobe). The line shown is a guide to the eye.

We have vacuum annealed Ni_3Pt films grown at various deposition temperatures for times from 4–100 h at 450°C , well below the order–disorder transition temperature and just slightly above the onset of significant bulk mobility, which is expected around $350\text{--}400^\circ\text{C} \sim T_{\text{m}}/3$, where T_{m} is the melting temperature [12]. Samples have also been annealed at 700°C , above the order–disorder transition. Samples grown at or below 400°C show a sharpened magnetic transition and a lower magnetic onset temperature after the anneal. Perpendicular anisotropy is reduced or eliminated (depending on annealing time and starting condition). Figs. 3d and e show $M(H)$ curves obtained at room temperature on the (111) and (100) Ni_3Pt samples grown at 385°C after annealing at 450°C for 4 h. Fig. 4 shows normalized $M(T)$ for the same (111) and (100) samples as-deposited, after annealing at 450, and after annealing at 700°C . For the (111) sample, K_{ui} is reduced to $\sim 3 \times 10^5 \text{ erg/cm}^3$ after a 4 h anneal, while in the (100) sample it is completely eliminated. For both samples, annealing at 725°C significantly reduces the magnetic onset temperature; annealing at 450°C causes a significant reduction in the (100) sample and very little change in the (111), despite the large change in anisotropy. Anisotropy thus vanishes faster with annealing than magnetic onset enhancement,

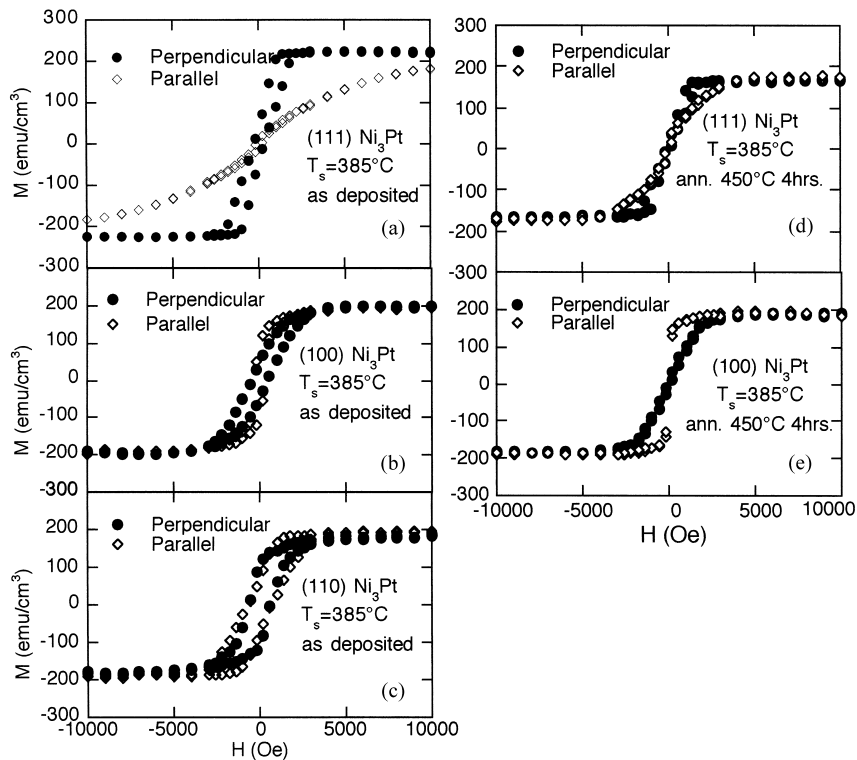


Fig. 3. $M(H)$ measured at 300 K with H perpendicular or parallel to the film plane for epitaxial Ni_3Pt (~ 73 at% Ni) grown at 385°C : (a) (111), (b) (100), and (c) (110), as deposited; (d) (111) and (e) (100) after annealing at 450°C for 4 h.

presumably due to different sensitivities to local arrangements. This effect was also seen in CoPt_3 ; there it was postulated that the Co/Pt platelet interfaces were roughened before the platelets completely vanished [12]. Ni_3Pt initially deposited at 650°C , above the L_{12} order–disorder transition, and annealed at 450°C shows a reduction in its onset temperature to below the FCC Curie temperature. From the magnetic data, it thus appears that growth-induced clustering in Ni_3Pt gradually vanishes with annealing at 450°C and samples develop partial LRO, as expected from the equilibrium phase diagram.

NiPt_3 is nonmagnetic in both the A1 (chemically disordered FCC) and L_{12} (LRO) bulk phases [24]. More precisely, it is paramagnetic in the A1 phase, with a very small moment per Ni atom (approximately $0.14\mu_B$), [34] and nearly certainly non-magnetic in the L_{12} phase due to the increased Ni–Ni separation in this phase. We have however found

that (111) and (100) oriented NiPt_3 films grown at 350°C show measurable magnetization with an onset at ~ 80 K and a broad magnetic transition. This observation is indicative of significant Ni clustering. After annealing at 600°C (above the LRO temperature) for 4 h, $M(H, T)$ dropped appreciably, to closer to the expected low paramagnetic signal. Fig. 5a shows $M(T)$ for the (100) and (111) samples, both as-deposited and after annealing, measured in 1000 Oe. Fig. 5b shows $M(H)$ measured at 10 K for the as-deposited samples; the annealed samples appear simply paramagnetic with lower susceptibility. The magnetization in the as-deposited state is small, and it is not clear from this data if there is a spontaneous magnetization at 10 K or not, but the induced magnetization is considerably larger than the equilibrium paramagnetic value which would not be visible on either plot (e.g. at 5 K, in 1000 Oe, M would be ~ 0.003 emu/cm³ for the A1 phase). $M(T)$ does not fit a simple Curie (or

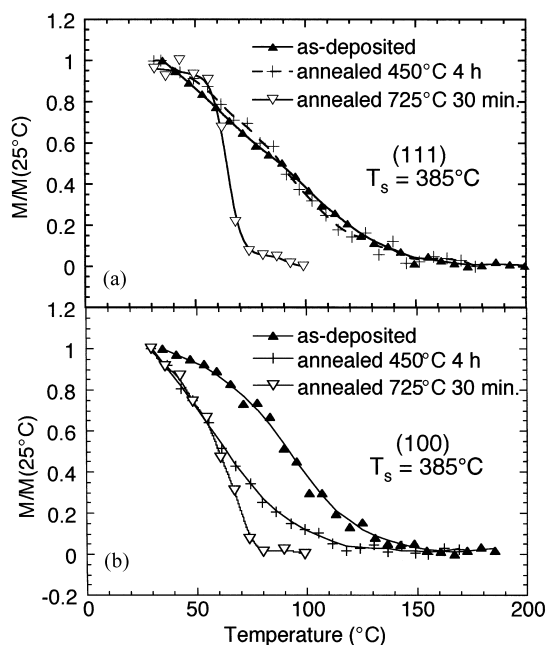


Fig. 4. Normalized $M(T)/M(25^\circ\text{C})$ for (a) (111) and (b) (100) Ni_3Pt (~ 73 at% Ni) grown at 385°C in the as-deposited state and after annealing at 450°C and 725°C as shown. Measurements to 400°C have no effect on the properties of the films.

Curie–Weiss) dependence; in addition, the value of μ required would be unreasonably large (of order $3\mu_{\text{B}}$ per NiPt_3 unit cell assuming a simple paramagnetic susceptibility at 10 K). It thus appears far more likely that NiPt_3 grown at 350°C is actually ferromagnetic in some regions of the sample but inhomogeneous with a very broadened onset temperature, as seen in the other compositions. In both $M(H)$ and $M(T)$, the high temperature $M(250\text{ K}, 1000\text{ Oe})$ was subtracted in order to remove background and substrate contributions, which are appreciable given the small signal. The differences between (100) and (111) orientations in $M(T)$ appear real but are close to the level of uncertainty in the measurement ($\pm 1 \times 10^{-5}$ emu). There is no anisotropy in either the as-deposited or annealed state for either orientation; specifically, perpendicular or parallel applied field gave the same $M(T)$ and $M(H)$. Demagnetizing effects are small compared to the applied field due to the low M .

NiPt films grown between 200°C and 400°C show significant clustering. Figs. 6a and b show

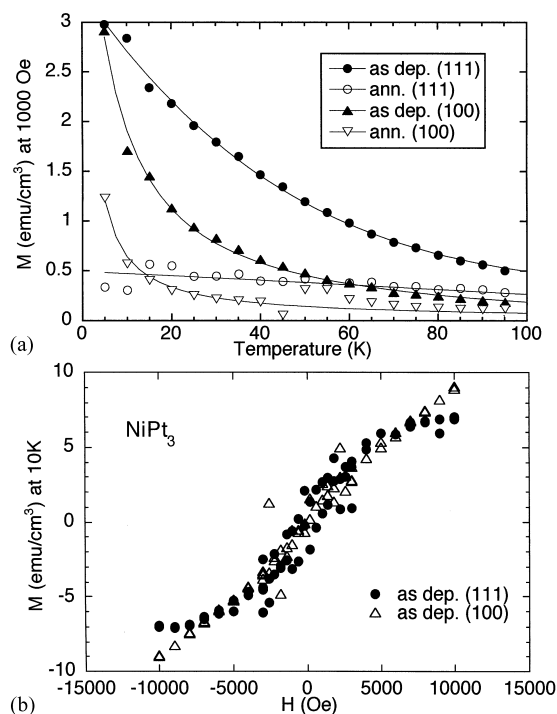


Fig. 5. (a) $M(T)$ measured in $H = 1000\text{ Oe}$ and (b) $M(H)$ measured at 10 K for (100) and (111) NiPt_3 grown at 350°C as-deposited and after annealing at 600°C (above the LRO temperature) for 4 h. Lines shown are a guide to the eye. After annealing, $M(H)$ for both samples is linear with a smaller susceptibility. The expected induced magnetization for FCC NiPt_3 would be 0.003 emu/cm^3 in 1000 Oe at 5 K.

normalized $M(T)/M(10\text{ K})$ measured in 1000 Oe for (100) and (111) oriented NiPt samples deposited at 200°C , 400°C , and 700°C both as-deposited and after annealing at 700°C (compositions differ slightly; $T_s = 200^\circ\text{C}$ and 400°C samples are ~ 47 at% Ni, while 700°C are 50 at% Ni). Samples deposited at 700°C (above the LRO temperature) have a sharp magnetic transition near the Curie temperature of FCC NiPt . Films grown between 200°C and 400°C exhibit broad transitions with enhanced magnetic onset temperature. After annealing at 700°C , all films exhibit sharp transitions, with a T_c appropriate to their composition, indicative of homogeneous FCC phase, as expected.

Samples of both orientations deposited at 600°C show a magnetic onset temperature of 70 K, significantly below that of FCC NiPt (115 K), due

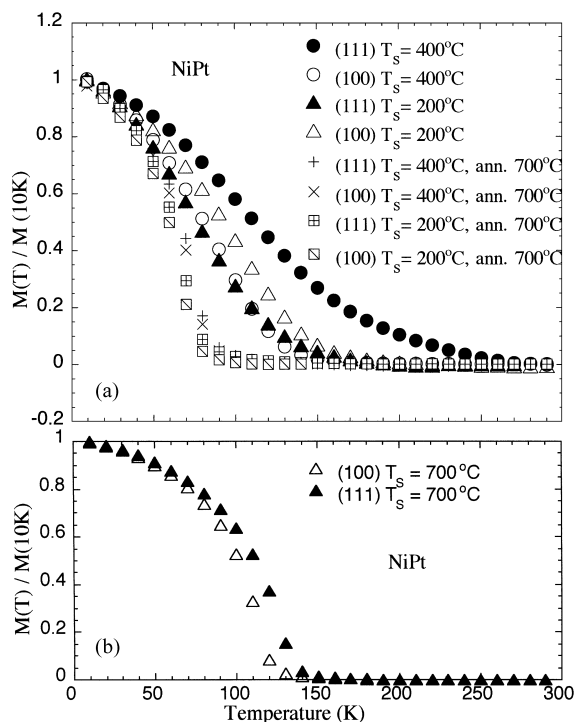


Fig. 6. (a) $M(T)/M(10K)$ for (111) and (100) NiPt samples deposited at 200°C and at 400°C as-deposited and after vacuum annealing at 700°C (above the LRO temperature) for four hours. Composition $x \sim 47$ at% Ni; FCC $T_c \sim 80$ K. M was measured with H applied along the easy axis/plane as measured at 10 K, after saturating in 10000 Oe. After annealing, the magnetic transition sharpens in all films and $M(T)$ of the annealed films look identical. (b) $M(T)/M(10K)$ for (111) and (100) NiPt deposited at 700°C; composition $x \sim 50$ at% Ni has FCC $T_c \sim 115$ K.

presumably to formation of partial LRO. (The LRO phase is paramagnetic at all temperatures.) Their saturation magnetization (~ 15 emu/cm³ measured at 10 K) is also suppressed well below the FCC value (~ 63 emu/cm³). Samples deposited at 500°C show intermediate behavior, with an ordering temperature near the expected FCC value, but significant broadening.

Clustering in NiPt is much larger for (111) films than for (100) films. This is unlike CoPt₃ where nearly identical behavior was found for all low index orientations. As seen in Fig. 6a, the (111) sample deposited at 400°C shows a particularly broad transition with a very large magnetic onset

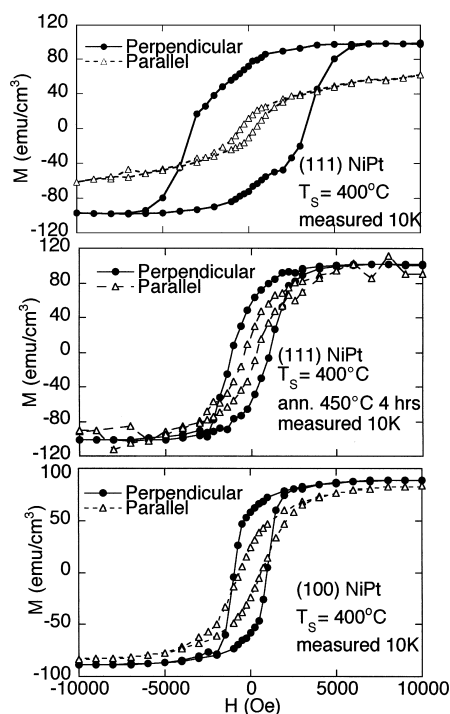


Fig. 7. $M(H)$ curves, with H parallel or perpendicular to the film plane, measured at 10 K for NiPt deposited at 400°C: (a) (111) as-deposited, (b) (111) after annealing at 450°C, and (c) (100) as-deposited. Anisotropy and coercivity in (a) are large and are much reduced in (b). After annealing at 450°C, the (100) sample is non-magnetic.

temperature enhancement. By contrast, the (100) NiPt film deposited at 400°C shows a magnetic transition which is only slightly broadened with a much smaller enhancement above the FCC Curie temperature. (100) and (111) films were grown simultaneously in a single deposition, so the difference is not attributable to compositional or other variations in growth; in addition, $M(T)$ is identical after annealing at 700°C, which eliminates memory of the growth process. Samples grown at 300°C show a similar orientation-dependent broadening and enhancement of $M(T)$. For samples grown at 200°C (see Fig. 6a), the differences are reversed with respect to orientation (i.e. (100) has higher onset than (111)) but the difference is small.

A large difference between (111) and (100) NiPt films is also seen in anisotropy and coercivity. Figs. 7a and c are plots of the parallel and perpendicular

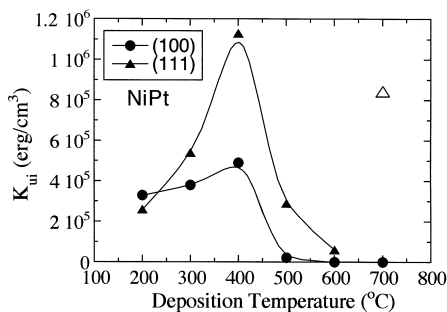


Fig. 8. Intrinsic, uniaxial perpendicular anisotropy K_{ii} at 10 K in as-deposited (100) and (111) oriented NiPt films as a function of substrate temperature during growth (shape anisotropy contribution removed). The anisotropy in the (111) film grown at 700°C is of a different nature (as discussed in the text) and is shown with an open triangle. The lines are a guide to the eye.

$M(H)$ loops measured at 10 K for (100) and (111) oriented NiPt films deposited simultaneously at 400°C. The (111) sample shows PMA and substantial hysteresis. Saturation magnetization (100 emu/cm³) is substantially enhanced over the FCC value (< 63 emu/cm³ for 47 at% Ni). Annealing at 450°C for 4 h (shown in Fig. 7b) reduces PMA to only slightly above shape anisotropy, consistent with this anisotropy being a growth-induced effect. The (100) sample deposited at 400°C (Fig. 7c) shows significantly less anisotropy, coercivity, and moment enhancement in the as-deposited state than the (111). After annealing at 450°C for 4 h, the (100) sample is non-magnetic, indicative of formation of LRO.

PMA for these films was measured at 10 K through extrapolation of the hard axis (or hard plane) hysteresis loop to H_K . The anisotropy $K_u = (H_K^* M_s)/2$ and the intrinsic PMA $K_{ui} = K_u + 2\pi M_s^2$ were then determined. Fig. 8 shows K_{ui} for (100) and (111) oriented NiPt films as a function of deposition temperature; the anisotropy is substantial for (111) films, and is much less for (100) films. A (111) sample grown at 400°C with slightly more Ni (Ni₅₂Pt₄₈) has PMA with $K_{ui} = 2.5 \times 10^6$ erg/cm³ measured at 150 K; after annealing, it is non-magnetic at 150 K. The (100) sample grown in the same run is magnetic in the as-deposited state at 150 K but with low PMA; it too is non-magnetic at 150 K after annealing at 450°C.

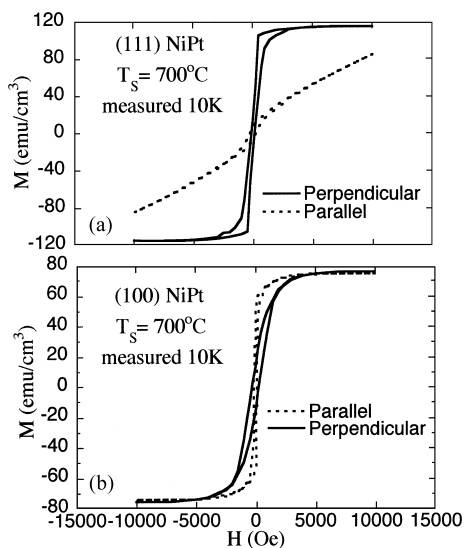


Fig. 9. $M(H)$ curves, with H parallel or perpendicular to the film plane, acquired at 10 K for as-deposited NiPt: (a) (111) and (b) (100) deposited at 700°C. The (111) has a perpendicular easy axis, but very low coercivity.

The (111) film grown at 700°C (but not the (100)) shows large perpendicular anisotropy, despite the fact that the $M(T)$ curves for both (100) and (111) NiPt films grown at 700°C indicate a simple homogeneous FCC structure (Fig. 6b). The anisotropy for this sample is shown in Fig. 8 by an open triangle as it is of significantly different character than the anisotropy of the other samples shown in Fig. 8. In addition to not being associated with enhanced broadened magnetization onset, it is not associated with coercivity and does not vanish with annealing at 450°C or 700°C, unlike the growth-induced effects described elsewhere in this paper. Figs. 9a and b show hysteresis loops (measured at 10 K) for (100) and (111) samples grown at 700°C. The (111) film grown at 700°C shows large PMA but small coercivity. Annealing at 450°C does not affect this PMA. In addition, (111) samples grown at 200°C or 400°C and then annealed at 700°C show these same anisotropy effects; representative data of $M(H)$ measured at 10 K are shown in Figs 10a and b. These (111) films grown at 200°C or 400°C have large anisotropy as-deposited; annealing at 450°C reduces/eliminates this

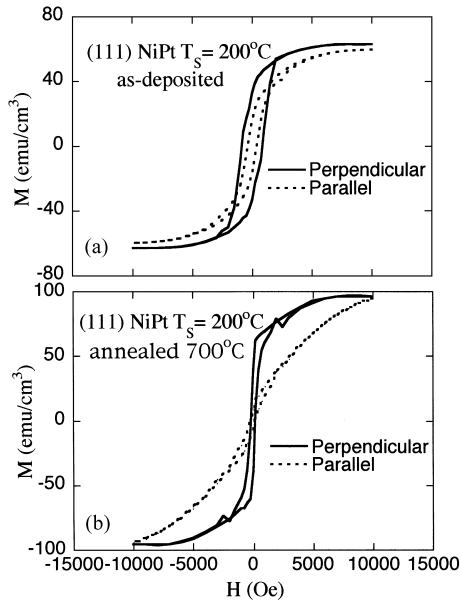


Fig. 10. $M(H)$ curves, with H parallel or perpendicular to the film plane, acquired at 10 K for (111) oriented NiPt film grown at 200°C (a) as-deposited and (b) after vacuum annealing at 700°C. (100) NiPt samples grown at either 200°C or 400°C and then annealed at 700°C show in-plane (shape) anisotropy only, with no coercivity, similar to Fig. 8b.

growth-induced anisotropy (dependent on annealing time), but then annealing at 700°C causes the non-growth-induced anisotropy to form. The magnitude of PMA in the (111) sample grown at 200°C (400°C) after annealing at 700°C is 5×10^5 (8×10^5) erg/cm³, very similar to 8×10^5 erg/cm³ for the as-deposited (111) sample grown at 700°C. (111) films either grown or annealed at 700°C also show an enhancement of their saturation magnetization M_s , although not of their T_c . By contrast, (100) oriented samples deposited or annealed at 700°C do not show any of these effects: they have the expected FCC M_s and T_c , and $M(H)$ loops show an easy plane with $H_K = 4\pi M_s$, no coercivity, or PMA. The similarity between (111) samples grown or annealed at 700°C suggest that this non-growth-induced PMA is an equilibrium effect, perhaps related to magnetostriction due to strain induced by differential thermal contraction of sample and substrate. We have measured in plane lattice constants by off axis X-ray diffraction ex-

periments. The deduced strain in the NiPt alloy is small, (0.5%) and tensile.

4. Discussion

As in Pt-rich Co–Pt alloys, the magnetic data suggest that Ni atoms are clustering in as-deposited samples of all three compositions when grown between 200°C and 400°C despite the fact that the equilibrium phase diagram indicates a homogeneous phase for all three, and despite the fact that they are structurally epitaxial single-crystal films. These samples show greatly broadened magnetic transitions with enhanced magnetic onset (up to 100°C higher than the FCC phases of these compositions), indicative of inhomogeneity and clustering of the Ni atoms. Clustering is eliminated by annealing and occurs only in this window of growth temperatures; both above and below, homogeneous FCC or LRO phases are formed. The observation that low-temperature growth produces a homogeneous material that eliminates the possibility of trivial explanations such as deposition rate fluctuations. For growth temperatures above 400°C, it is possible that clustering still occurs at the surface during growth but is annealed away as the deposition continues due to appreciable bulk atomic mobility. A particularly striking example of clustering is the magnetization seen in NiPt₃ deposited at 350°C. The magnitude of the moment of Ni is very susceptible to environmental effects; usually, Ni must have at least three Ni neighbors to possess a moment at all [24]. As a result, homogeneous NiPt₃ even in the FCC phase barely possesses a moment and does not magnetically order, and the LRO L1₂ phase is non-magnetic [24,34]. Thus, only significant Ni clustering could produce the magnetization we have measured in NiPt₃ films.

Perpendicular magnetic anisotropy, coercivity and remanence is found in as-deposited NiPt and Ni₃Pt samples grown between 200°C and 400°C; like the clustering, anisotropy is eliminated by annealing at temperatures as low as 450°C. A significant difference is seen in the extent of clustering and anisotropy for (111) and (100) Ni–Pt films. In Co–Pt, no difference was found between any of the

low index orientations ((100), (110), (111), and polycrystalline with (111) texturing) [12]. For Ni_3Pt , PMA is appreciable even at room temperature, increases at lower T , and is much larger in (111)-oriented films than in (100). Similarly, (111) NiPt films show much larger anisotropy than (100) (both measured at 10 K due to their low ordering temperature). Insufficient work has been done to permit a general statement about the (110) orientation, but for Ni_3Pt , (110) samples appear similar to (100). For (111) NiPt, as well as to a lesser extent (100) NiPt, the *magnitude* of the growth-induced PMA, not just its presence or absence, correlates well with the value of the magnetic onset temperature, as seen in CoPt_3 [12]. This correlation is also seen in Ni_3Pt , but is less striking; specifically, the magnetic onset temperature depends on orientation, but less strongly than in NiPt.

For Ni_3Pt , both the A1 and L1_2 phases are cubic, hence PMA must be a consequence of local ordering, caused by the growth process. For NiPt, where LRO leads to a tetragonal L1_0 structure, this is in principle a possible source of PMA. There are however many arguments against this. First, partial chemical LRO is hard to reconcile as the mechanism for PMA in (111) oriented samples, when it is much smaller in (100) oriented samples, since L1_0 ordering occurs along the (100) orientation. Secondly, the presence of even partial LRO should reduce the magnetic ordering temperature, while these samples have an enhanced magnetic onset, indicative of clustering rather than LRO. Thirdly, annealing at 450°C eliminates the anisotropy (both for NiPt and Ni_3Pt), but should only act to increase any LRO present. We suggest instead that the growth-induced PMA for both NiPt and Ni_3Pt results when Ni clusters into platelets in a Pt-rich matrix, at the surface as the film grows, hence parallel to the substrate. This atomic arrangement results in a structure locally similar to a multilayer but incoherent across the sample, so that X-ray measurements see only the (long range) FCC structure.

The appearance of Ni platelets in a material with a negative chemical energy of mixing (favoring ordering, not separation) is unexpected. Magnetic energy has been suggested to give rise to a low-temperature phase separation in hexagonal Co–Cr

alloys, but here seems unlikely to be the responsible mechanism, as the samples with the greatest clustering and anisotropy (those deposited at 400°C) are deposited above the Curie temperature of bulk Ni (363°C), and well above the Curie temperature of any of the alloys. We suggest instead that the Ni platelets are formed as a result of surface equilibrium effects, important for all compositions but dependent on the surface structure and hence different for the (111) and the (100) surfaces. Previous workers, including ourselves, have suggested an interplay between surface equilibrium effects and rapid surface diffusion but limited bulk atomic mobility as being the driving force in producing clustering and perpendicular anisotropy [7,8,12,14]. Surface segregation for example could cause clustering into platelets in the (111) orientation, where the surface is known to be flat. In the absence of significant bulk atomic mobility, the surface arrangement would be ‘frozen’ in the as-deposited sample due to subsequently deposited layers of material.

The reduced clustering and PMA in (100) NiPt and Ni_3Pt relative to (111) may be related to differences in equilibrium surface structure. The surface of (100) oriented NiPt is known to have a ‘shifted row’ reconstruction with every fifth row being significantly shifted out of the plane [30]. This could break up the formation of platelets on the surface. By contrast, the (100) CoPt_3 surface undergoes a quasi-hexagonal reconstruction that leaves it flat [32], and similar to the (111) surface, perhaps explaining why there is no significant orientational dependence of the clustering or anisotropy in Co–Pt films [12].

The presence of perpendicular anisotropy in (111) oriented NiPt films deposited or annealed at 700°C (above the LRO temperature) is not yet understood, but we note that it is quite unlike the anisotropy found in films grown at 400°C . Rather than vanishing with annealing, like the growth-induced effects, it is found equally in (111) samples annealed or deposited at 700°C . It is also not associated with a magnetic ordering temperature enhancement, a broadened magnetic transition, or significant coercivity. For (100) NiPt samples, the (small) growth-induced PMA seen in as-deposited samples grown between 200°C and 400°C relaxes

away on annealing at 450°C or 700°C. However, for the (1 1 1) samples, the magnitude of PMA is not monotonic in annealing temperature. It drops with annealing at 450°C, but recurs on annealing at 700°C, independent of original growth temperature. The identical sharp shape of the magnetic transition and Curie temperatures of all samples grown or annealed at 700°C (despite very different initial $M(T)$) suggests that samples have reached an equilibrium state at 700°C. Further work is needed to identify the underlying structural cause of the anisotropy, but differential thermal contraction-induced strain is a possibility. The measured strain is small (0.5%) and tensile, consistent with differential thermal contraction. To the best of our knowledge, magnetostriction coefficients have not been measured for Ni–Pt alloys. However, in thin Ni/Pt multilayers, where magnetostriction coefficients have been measured [23], the authors conclude that perpendicular anisotropy in the multilayers is a result of the magnetoelastic anisotropy due to the tensile stress in the Ni sublayer. In the absence of magnetostriction coefficients data for NiPt alloys and in analogy with the multilayer system, we conjecture that the tensile strain measured in our NiPt(1 1 1) alloy film could perhaps also lead to perpendicular anisotropy as seen in Fig. 8.

5. Summary

We have vapor deposited epitaxial (1 0 0), (1 1 0), (1 1 1), and polycrystalline Ni₃Pt, NiPt, and NiPt₃ films over a range of growth temperatures from 80°C to 700°C. Films grown at temperatures above approximately 500°C form in equilibrium structures (chemically disordered FCC or chemically ordered LRO phases, depending on the growth temperature). Films grown at low temperatures (e.g. 80°C) are simple chemically disordered FCC, with the associated simple magnetic properties. This low-temperature FCC phase formation is presumably a result of limited surface atomic mobility during growth, which kinetically suppresses formation of the equilibrium long-range order phases.

At intermediate growth temperatures (between 200°C and 450°C), where surface atomic mobility is high but bulk atomic mobility is low, films of all

three compositions show magnetic signatures of Ni clustering. These signatures include enhanced and broadened magnetic onset temperature, enhanced low-temperature magnetization, perpendicular anisotropy, and coercivity, similar to what was previously seen in CoPt₃. These growth-induced properties vanish with annealing at or above 450°C. The clustering occurs on a local scale and is not visible in X-ray diffraction, which sees a simple chemically disordered FCC.

There is a significant difference in clustering and anisotropy between (1 0 0) and (1 1 1)-oriented films which was not seen in CoPt₃. This difference is suggested to be related to different reconstructions of the growth surface. As in Co–Pt alloys, the enhanced magnetic onset temperature, saturation magnetization, coercivity and perpendicular anisotropy are consistent with flat platelet-like layering between Ni and Pt on the growth surface, perhaps due to a frustrated surface segregation. We suggest that the local morphology of the growth surface plays a critical role in the formation of these platelets, with non-flat surfaces such as the shifted row (1 0 0) suppressing clustering and hence anisotropy.

Additional work is needed to understand the source of perpendicular anisotropy in (1 1 1) NiPt films deposited or annealed at 700°C.

Acknowledgements

We would like to thank D. Weller for valuable discussions concerning models, and P. Larraburre, S. Kim and I.K. Schuller for help with the X-ray diffractometer. This work was supported by DOE Grant No. DE-FG03-95ER45529, by the University of California Campus Laboratory Collaboration, and by the DOD-MURI (F49620-96-1-0026), and benefited from the use of facilities provided by the Center for Magnetic Recording Research and by the Center for Interface and Materials Science at UCSD.

References

- [1] R.F.C. Farrow, R.F. Marks, A. Cebollada, G.R. Harp, T.A. Rabedeau, M.F. Toney, D. Weller, S.S.P. Parkin, J. Crystal Growth 150 (1995) 1126.

- [2] C.J. Lin, G. Gorman, *Appl. Phys. Lett.* 61 (1992) 1600.
- [3] D. Weller, H. Brandle, G. Gorman, C.-J. Lin, H. Notarys, *Appl. Phys. Lett.* 61 (1992) 2726.
- [4] D. Weller, H. Brandle, C. Chappert, *J. Magn. Magn. Mater.* 121 (1993) 461.
- [5] E.E. Marinero, R.F.C. Farrow, G.R. Harp, R.H. Geiss, J.A. Bain, B. Clemens, *Mat. Res. Soc. Symp. Proc.* 313 (1993) 677.
- [6] R.F.C. Farrow, D. Weller, M.F. Toney, T.A. Rabedeau, J.E. Hurst, G.R. Harp, R.F. Marks, R.H. Geiss, H. Notarys, *Mat. Res. Soc. Symp. Proc.* 343 (1994) 375.
- [7] P.W. Rooney, A.L. Shapiro, M.Q. Tran, F. Hellman, *Phys. Rev. Lett.* 75 (1995) 1843.
- [8] M. Maret, M.C. Cadeville, R. Poinot, A. Herr, E. Beaurepaire, C. Monier, *J. Magn. Magn. Mater.* 166 (1997) 45.
- [9] Li Ming, Jiang Zhihong, Zou Zhiqiang, Shen Defang, *J. Magn. Magn. Mater.* 176 (1997) 331.
- [10] Y. Yamada, T. Suzuki, E.N. Abarra, *IEEE Trans. Magn. MAG33* (1997) 3622.
- [11] W. Grange, M. Maret, J.-P. Kappler, J. Vogel, A. Fontaine, F. Petroff, G. Krill, *Phys. Rev. B* 58 (1998) 6298.
- [12] A.L. Shapiro, P.W. Rooney, M.Q. Tran, F. Hellman, K.M. Ring, K.L. Kavanagh, B. Rellinghaus, D. Weller, *Phys. Rev. B* 60 (1999) 12826.
- [13] G.R. Harp, D. Weller, T.A. Rabedeau, R.F.C. Farrow, M.F. Toney, *Phys. Rev. Lett.* 71 (1993) 2493.
- [14] M. Maret, M.C. Cadeville, A. Herr, R. Poinot, E. Beaurepaire, S. Lefebvre, M. Bessiere, *J. Magn. Magn. Mater.* 191 (1999) 61.
- [15] J. Bain, B. Clemens, S. Brennan, *Mat. Res. Soc. Symp. Proc.* 312 (1993) 291.
- [16] F. Hellman, A.L. Shapiro, E.N. Abarra, P.W. Rooney, M.Q. Tran, in *MORIS conference proceedings*, *J. Magn. Soc. Japan* 23 (Suppl. S1) (1999) 79.
- [17] T.A. Tyson, S.D. Conradson, R.F.C. Farrow, B.A. Jones, *Phys. Rev. B* 54 (1996) 3702.
- [18] C. Meneghini, M. Maret, M.C. Cadeville, J.L. Hazemann, *J. Phys. IV Colloq.* 7 (1997) C2–1115.
- [19] C. Meneghini, M. Maret, V. Parasote, M.C. Cadeville, J.L. Hazemann, R. Cortes, S. Colonna, *Eur. Phys. J. B* 7 (1999) 347.
- [20] R. Krishnan, H. Lassri, M. Porte, M. Tessier, P. Renaudin, *Appl. Phys. Lett.* 59 (1991) 3649.
- [21] P. Pouloupoulos, M. Angelakeris, D. Niarchos, N.K. Flevaris, *J. Magn. Magn. Mater.* 140 (1995) 613.
- [22] M. Angelakeris, P. Pouloupoulos, N. Vouroutzis, M. Nyvly, V. Prosser, S. Visnovsky, R. Krishnan, N.K. Flevaris, *J. Appl. Phys.* 82 (1997) 5640.
- [23] Young-Soek Kim, Sung-Chul Shin, *Phys. Rev. B*, 59, (1999) R6597.
- [24] C.E. Dahmani, M.C. Cadeville, J.M. Sanchez, J.L. Moran-Lopez, *Phys. Rev. Lett.* 55 (1985) 1208.
- [25] M. Hansen, K. Anderko, *Constitution of Binary Alloys*, McGraw-Hill, New York, 1958.
- [26] S. Deckers, F.H.P.M. Habraken, W.F. van der Weg, A.W. Denier van der Gon, B. Pluis, J.F. van der Veen, R. Baudoin, *Phys. Rev. B* 42 (1990) 3253.
- [27] Y. Gauthier, R. Baudoin, Y. Joly, J. Rundgren, J.C. Bertolini, J. Massardier, *Surf. Sci.* 162 (1985) 342.
- [28] Y. Gauthier, R. Baudoin, M. Lundberg, J. Rundgren, *Phys. Rev. B* 35 (1987) 7867.
- [29] E. van de Riet, S. Deckers, F.H.P.M. Habraken, A. Niehaus, *Surf. Sci.* 243 (1991) 49.
- [30] M. Schmid, A. Biedermann, S.D. Bohmig, P. Weigand, P. Varga, *Surf. Sci.* 318 (1994) 289.
- [31] S. Deckers, F. Bischof, D. de Jager, S.H. Offerhaus, J. van Roijen, F.H.P.M. Habraken, W.F. van der Weg, *Surf. Sci.* 258 (1991) 82.
- [32] U. Bardi, A. Atrei, P.N. Ross, E. Zanazzi, G. Rovida, *Surf. Sci.* 211–212 (1989) 441.
- [33] A.L. Shapiro, Ph.D. Thesis, 1999.
- [34] R.M. Bozorth, *Ferromagnetism* Nostrand Co., Princeton, 1978, p. 440.